Electronic Supplementary Material (ESI) for Physical Chemistry Chemical Physics.

# Supplementary Information

# Redox Titration of Gold and Platinum Surface Oxides at Porous Microelectrodes

Mareike Haensch[a,†], Julian Behnken[a,b,†], Luis Balboa[a], Alexander Dyck[b], Gunther Wittstock[a,*]

[a] *Carl von Ossietzky University, Institute of Chemistry, Carl-von-Ossietzky-Str. 9-11,*
*26129 Oldenburg, Germany.*

[b] *DLR Institute of Networked Energy Systems, Carl-von-Ossietzky-Str. 15,*
*26129 Oldenburg, Germany.*

## S1: Digital simulation of surface interrogation mode extended to porous microelectrodes

Simulations of the titration of the oxides adsorbed at the surface of the porous electrodes were developed using COMSOL Multiphysics version 5.3 (COMSOL Inc. Burlington, MA). A 2D axisymmetric geometry was used to describe the system depicted in Figure 1. The porous domain of the electrode was approximated by generating intercalated concentric lamella which represent the ligaments and the liquid phase of the porous electrode (Figure S1, not to scale). Ligament and pore size are equal (50-100 nm wide). The COMSOL report is provided as separate PDF document.

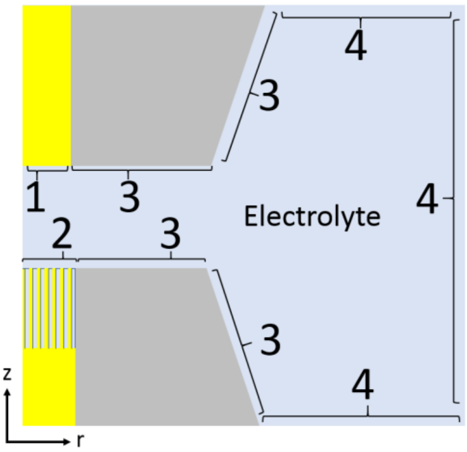

Fig S1: Schematic diagram of the simulation space. Box size for the electrolyte boundaries is 500 times the tip radius.

### Domain equations and boundary conditions

### Diffusion in the electrolyte

Mass transport in the electrolyte due to convection and migration was neglected. The diffusion equation in cylindrical coordinates is given in eq. (SI-1), where $c_i(r,z,t)$ is the mediator concentration ($i = O, R$) in its oxidized and reduced form. $D_i$ is the diffusion coefficient of the mediator assumed equal for both redox species.

$$\frac{\partial c_i}{\partial t} = D_i\left(\frac{\partial^2 c_i}{\partial r^2} + \frac{1}{r}\frac{\partial c_i}{\partial r} + \frac{\partial^2 c_i}{\partial z^2}\right) \qquad \text{(SI-1)}$$

### 1-microelectrode electrode flux

The microelectrode (ME) was modeled using Butler-Volmer kinetics with an overpotential ($E_T - E_0$) of -0.5 V ensuring diffusion-controlled reduction of the redox mediator. The ME used to titrate the substrate had a radius $r_T$ = 25µm.

$$\frac{\partial c_{\mathrm{O}}}{\partial t} = -c_{\mathrm{O}} k_0 \mathrm{e}^{-\left(\frac{\alpha F}{RT}(E-E_0)\right)} + c_{\mathrm{R}} k_0 \mathrm{e}^{-\left(\frac{(1-\alpha)F}{RT}(E-E_0)\right)} \qquad \text{(SI-2)}$$

$$\frac{\partial c_{\mathrm{R}}}{\partial t} = -(-c_{\mathrm{O}} k_0 e^{-\left(\frac{\alpha F}{RT}(E\text{-}E_0)\right)} + c_{\mathrm{R}} k_0 e^{-\left(\frac{(1\text{-}\alpha)F}{RT}(E\text{-}E_0)\right)}) \qquad \text{(SI-3)}$$

Where $k_0$ is the standard heterogeneous rate constant, α is the transfer coefficient, F the Faraday constant, R the gas constant, T the temperature. E the electrode potential, $E_0$ the standard potential.

**2-Porous substrate**

Two different oxides adsorbed at the porous electrode surface were modelled. The first oxide (Ox1) being adsorbed directly at the surface of the porous electrode and the second one (Ox2) being adsorbed on top of Ox1. Under this assumption that Ox2 reacts first with the mediator and only when there is less than one monolayer (ML) of Ox2 present ( $\theta_2 \leq 1$ ), Ox1 become accessible for the mediator.

The term $D_{\mathrm{Ox1,2}} \nabla^2 \Gamma_{1,2}$ on the right side of equations SI-6 and SI-7 represent the surface diffusion of the adsorbed oxides. The diffusion coefficient in this case was 100 times the value of the redox mediator in the solution ( $5.5\times10^{-8}\mathrm{m^2s^{-1}}$ ). This setting was used by Rodriguez-Lopez et al.$^1$. It avoids running into numerical inconsistencies which arise when the diffusion of the oxides is set to $0\ \mathrm{m^2s^{-1}}$. This assumption also ensures a homogeneous surface concentration of both oxides throughout the experiment. This effect is comparable to having a conductive substrate in which the potential is homogenous across the porous electrode surface. We tried to explicitly define an open circuit potential for the conductive porous electrode surface, however we have not yet been able to overcome the numerical challenges mentioned above. However, the approach of setting a high diffusion coefficient for the adsorbed oxides seems as a good approximation for the vertical electron transfer discussed in the main text.

We chose to use the surface coverage ($\Theta_i$) instead of the surface concentration ($\Gamma_i$) directly for the reaction rate. At values above 1 ML, $\Theta_i$ keeps a value of 1 as we assume the maximum amount of oxide that can be in contact with the mediator is 1.

The factor ($\Theta_1$-$\Theta_2$) that precedes the Ox1 reaction with the mediator guarantees that only the outer oxide reacts with the mediator if its surface coverage is larger than that of the Ox2.

The substrate has a radius of 25 µm with depths varying from 8 to 16 µm.

*Reaction rate redox mediator at the substrate*

$$\frac{\partial c_{\mathrm{O}}}{\partial t} = (\theta_1 \text{-} \theta_2) k_{\mathrm{ox1}} c_{\mathrm{R}} + \theta_2 k_{\mathrm{ox2}} c_{\mathrm{R}} \qquad \text{(SI-4)}$$

$$\frac{\partial c_{\mathrm{R}}}{\partial t} = -((\theta_1 - \theta_2) k_{\mathrm{ox1}} c_{\mathrm{R}} + \theta_2 k_{\mathrm{ox2}} c_{\mathrm{R}}) \qquad \text{(SI-5)}$$

*Reaction rate oxide 1*

$$\frac{\partial \Gamma_1}{\partial t} = (\theta_1 - \theta_2) k_{\mathrm{ox1}} c_{\mathrm{R}} + D_{\mathrm{ox1}} \nabla^2 \Gamma_1 \qquad \text{(SI-6)}$$

*Reaction Rate oxide 2*

$$\frac{\partial \Gamma_2}{\partial t} = \theta_2 k_{ox2} c_r + D_{ox2} \nabla^2 \Gamma_2 \qquad \text{(SI-7)}$$

$$\theta_1 = \min(\frac{\Gamma_1}{\Gamma_{\max}},1) \;\; \theta_2 = \min(\frac{\Gamma_2}{\Gamma_{\max}},1) \qquad \text{(SI-8)}$$

*Glass Insulator*

$$\frac{\partial c_{\mathrm{O}}}{\partial t} = 0 \, , \; \frac{\partial c_{\mathrm{R}}}{\partial t} = 0 \qquad \text{(SI-9)}$$

*Bulk*

$$c_{\mathrm{O}} = c_{\mathrm{O}}^{\mathrm{bulk}} \qquad \text{(SI-10)}$$

$$c_{\mathrm{R}} = 0 \qquad \text{(SI-11)}$$

*Current at the tip*

The ME current was calculated using:

$$i_{\mathrm{tip}} = 2\pi F D_{\mathrm{O}} \int_{r=0}^{r=\mathrm{rt}} \frac{\partial c_{\mathrm{O}}}{\partial z} r \, dr \qquad \text{(SI-12)}$$

### S2: Cyclic voltammetry of NPG-CME and Pt/C-CME in sulfuric acid and phosphate buffer solution

Cyclic voltammetry (CV) were recorded in 0.5 M phosphate puffer on a NPG-CME and a Pt/C-CME to select the potentials for oxide generation in SI-SECM experiments (Fig. S2 and S3). For comparison, CV in 0.1 M $H_2SO_4$ are shown as well. Slight changes of the oxide formation process are observable. Furthermore, for Pt/C-CME the hydrogen adsorption/desorption area is distorted in phosohate buffer solution. All reported $A_{\mathrm{ECSA}}$ values in the main text refer to CVs in 0.1 M $H_2SO_4$.

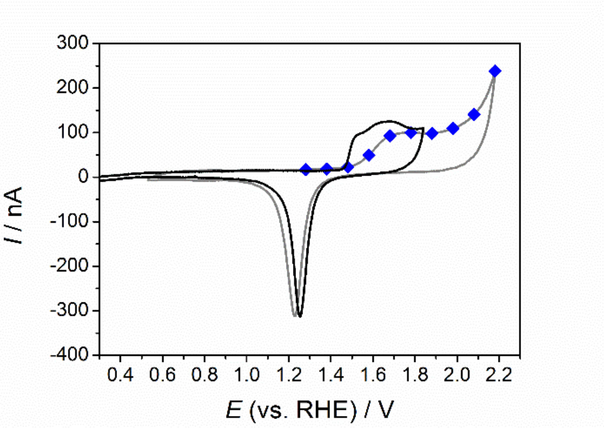

Fig S2: CV at NPG-CME in 0.1 M $H_2SO_4$ (black) or 0.5 M phosphate buffer (grey) with a scanrate of 100 mV/s. Blue diamonds indicate potentitals of oxide formation in SI SECM experiments reported in the main text.

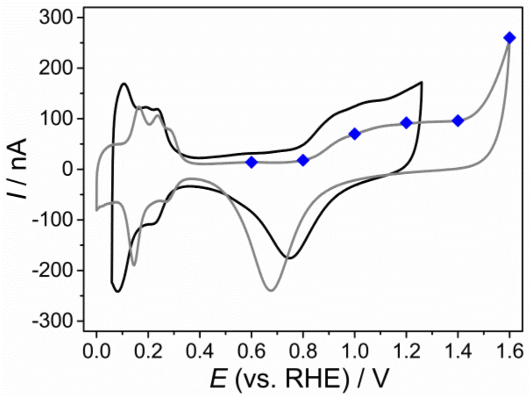

Fig. S3: CV at Pt/C-CME$_{17\mu m}$ in 0.1 M $H_2SO_4$ (black) or 0.5 M phosphate buffer (grey) with a scanrate of 50 mV/s. Blue diamonds indicate potentitals of oxide formation.

## S4: Cyclic voltammetry and surface interrogation mode of carbon black

A CME was filled with carbon black (CB, Vulcan® XC72R) to perform CV in 0.1 M $H_2SO_4$. The amount of surface oxides was estimated by calculating the charge of hydroquinone/quinone peaks at 0.6 V (Fig. S4a). This resulted in a charge of ca. 10 nC. Analogous to results shown in Fig. 7c (main manuscript), a SI-SECM experiment was performed with a CB-$CME_{15\mu m}$ of the same cavity depths. No oxide formation was detectable for the current transients at a generation potential of 0.6 – 1.0 V (Fig. S4b, curve 1-3). A peak appears at a potential of 1.2 V which increased with higher potentials. Charges were calculated by integration of current transients and subtraction of the charge of the background current controlled by hindered mediator diffusion (Fig. S4b, curve 1). Charges were between 0.2 µC at 1.2 and 1.4 V and 0.9 µC at 1.6 V as plotted in the inset of Fig. S4b. These charges results from surface oxide at the CB material as well as from background processes described in the main text.

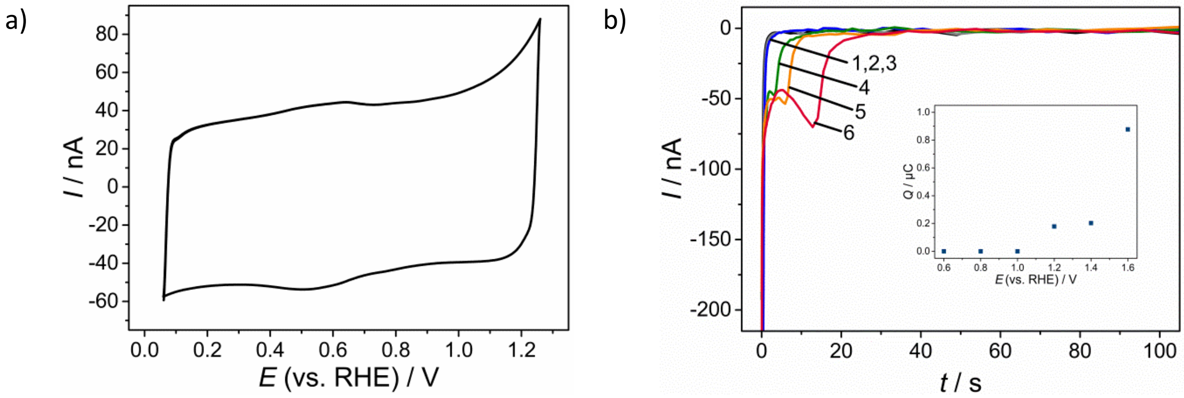

Fig. S4: a) CV of CB-$CME_{15\mu m}$ in 0.1 M $H_2SO_4$ with 200 mV/s and b) Titration curves of CB-$CME_{15\mu m}$ in 10 mM $[Ru(NH_3)_6]Cl_3$ + 0.5 M phosphate buffer (analogous to Fig. 7c). Numbers indicate the oxide generation potentials (2) 0.8 V; (3) 1.0 V; (4) 1.2 V; (5) 1.4 V and (6) 1.6 V applied for 60 s. The current transient from the sample without prior oxide formation (1) was used as background for the integration of currents.

## References

(1) J. Rodriguez-Lopez, A. Minguzzi and A. J. Bard, *J. Phys. Chem. C*, 2010, **114**, 18645–18655